Journal of Glaciology, Vol. 39, No. 131, 1993

A topological approach to the strain-rate pattern of ice sheets

J. F. Nye
H. H. Wills Physics Laboratory, University of Bristol, Bristol BS8 1TL, England

ABSTRACT. The pattern of horizontal strain rate in an ice sheet is discussed from a topological point of view. In a circularly symmetric ice sheet, the isotropic point for strain rate at its centre is degenerate and structurally unstable. On perturbation the degenerate point splits into two elementary isotropic points, each of which has the lemon pattern for the trajectories of principal strain rate. Contour maps of principal strain-rate values are presented which show the details of the splitting.

1. INTRODUCTION

The traditional way of applying mathematics to understand the flow of ice sheets is first to create a mathematical model. This will embody various assumptions about the form of the bed, whether it is hard or deformable, the flow law of the ice, whether it is isotropic and homogeneous, the thermal conditions, the accumulation rate and so on. The model is an idealization of nature. However, perhaps surprisingly, it is possible to make certain non-trivial and detailed mathematical statements about ice sheets that are quite independent of models of this kind.

Naturally, there has to be *some* connection between the mathematics and reality, but in the approach that I want to describe it is of a much more general kind than is found in the usual models. It can be stated very simply. If we consider an ice sheet — it could be the Antarctic or the Greenland ice sheet, or a past ice sheet — and make a topographic map of its surface, we are really making a model, because our map is a smoothed version of the real object. Similarly, if we consider the velocity distribution and make maps of it, the act of mapping is to make a model, namely a smoothed velocity distribution. It is these smoothed versions of reality, models if you like, that I want to discuss. The essential purpose of the smoothing operation is to allow certain rather general mathematical results about smooth functions to be applied.

The generality of the conclusions is both their strength and their weakness. In this respect, they are like results in thermodynamics: the price one pays for universality is that the results do not predict the magnitudes of physical quantities, but they do provide relations between them. Conventional model ice sheets, just because they have to be based on restrictive assumptions, cannot do justice to the full unsymmetrical generality of nature's ice sheets, with all their topographical complexity. However, topological reasoning can indicate the kind of behaviour that must occur even in the most complicated of situations. Thus, topological reasoning can complement the conventional approach.

In two recent papers, I have applied these ideas to the behaviour of the edge of an ice sheet (Nye, 1990) and to the distributions of ice velocity and strain rate in the neighbourhood of ice centres, that is, centres of flow (Nye, 1991). Here, I want to add a little more on the second of those topics.

2. ISOTROPIC POINTS

On a suitable scale of smoothing, the surface contours of an ice sheet around any one of its summits will approximate ellipses; this follows simply from the fact that the height of the surface can be expanded around the summit as a polynomial. The distribution of the horizontal component of instantaneous velocity defines a pattern of instantaneous flowlines (Nye, 1991) and, because we expect flow to be roughly perpendicular to the contour lines, we expect that the flowlines will spring outwards from a point that is normally very close to the summit. Let us consider now the corresponding pattern of horizontal strain-rate trajectories, that is, the two orthogonal families of curves whose directions at each point are the directions of the two principal components of horizontal strain rate.

We can obtain some insight into how they might behave by starting with the case of an ice sheet that has perfect circular symmetry in all its features (topography, accumulation rate, temperature, bed roughness, etc.). In such an ice sheet the distribution of horizontal strain rate must be circularly symmetrical. In the simplest case, the trajectories of principal strain rate would simply be radial lines and concentric circles (Fig. 1a). However, since circular symmetry is the only restriction, in the most general case the trajectories would be spirals, as indicated in Figure 1b. The spiral character of the pattern may only

https://doi.org/10.3189/S0022143000015677 Published online by Cambridge University Press

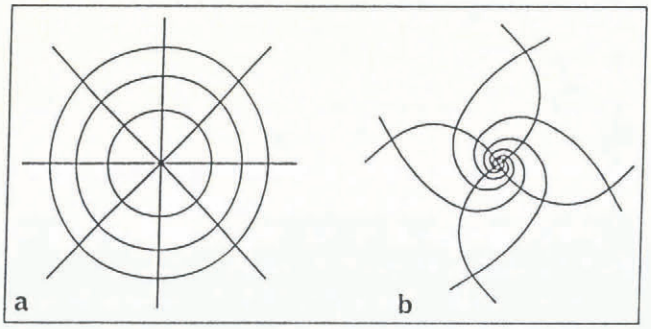

Fig. 1. Trajectories of principal horizontal strain rate in a circularly symmetrical ice sheet. (a) Simplest case. (b) With a spiral character.

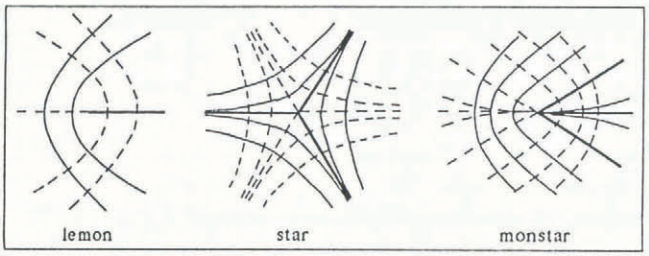

Fig. 2. The three possible structurally stable patterns of principal strain-rate trajectories around an isotropic point. The nomenclature is due to Berry and Hannay (1977).

be very slight but it is essential to include it to ensure generality in the argument.

An isotropic point for horizontal strain rate is defined quite generally as one where the two principal strain rates are equal, and isotropic points, in general, are not located at summits. It may be observed that the pattern of Figure 1b is quite unlike any of the three possible patterns of principal strain-rate trajectories around a generic (typical) isotropic point for strain rate (Nye, 1983). These are shown in Figure 2a, b and c, and none of them has circular symmetry. These patterns are structurally stable — in other words, although, when perturbed, they may move and distort, they will nevertheless retain their identities and will not break up or disappear.

The main difference between the various patterns in Figures 1 and 2 is captured by the notion of *singularity index*. This is defined in the following way. Make a clockwise circuit around the central singular point in any of the patterns and note how the strain-rate directions rotate as the circuit is traversed. They must rotate by a multiple of π to ensure continuity. If they rotate by $+2\pi$, as in Figure 1a and b, the singularity index is defined as $+1$; if they rotate by $+\pi$ as in Figure 2a and c, the index is $+\frac{1}{2}$; if they rotate by $-\pi$ as in Figure 2b, the index is $-\frac{1}{2}$. Thus, the difference between the symmetrical patterns of Figure 1a and b and the general patterns of Figure 2a, b and c is that the index is $+1$ rather than $\pm\frac{1}{2}$. Now, it is readily proved that singularity index, being a topological property, is a conserved quantity. Therefore, we expect that the patterns of Figure 1a and b will be unstable to perturbation, and, when perturbed in the most general possible way, they will break up into some combination of those of Figure 2a, b and c. The simplest combination is a pair of $+\frac{1}{2}$ points.

This expectation is confirmed by an analytical treatment (Nye, 1991). A typical splitting is shown in Figure 3, where two separated isotropic points both have the lemon pattern of Figure 2a. From each isotropic point there emerges a single trajectory of each orthogonal family, and it does not pass through the other isotropic point. That is, to say, the two isotropic points do not share a trajectory. That this occurs, even in a first-order perturbation, is a result of allowing a spiral character in the unperturbed pattern. Note that even the smallest trace of spirality, which will invariably exist, produces this result.

As the perturbation is increased, the two points will move further apart and first-order perturbation theory may cease to be applicable. Eventually, they may interact with other isotropic points which have moved in from the boundary of the ice sheet (this is possible because the circuit definition breaks down for an isotropic point on a boundary) or, alternatively, which have been created in pairs of opposite index (in fact, star + monstar).

With a given summit, with its elliptical rather than circular contours, it is an interesting question whether the pair of elementary istotropic points calculated by first-order perturbation will have made further interaction with other isotropic points or not. The answer will depend on the degree of smoothing that was used to construct the strain-rate distribution; for, in general, more smoothing means fewer isotropic points, and therefore fewer interactions. However, in all cases, provided new isotropic points have not entered from the boundary, the sum of the singularity indices of all the isotropic points must remain $+1$.

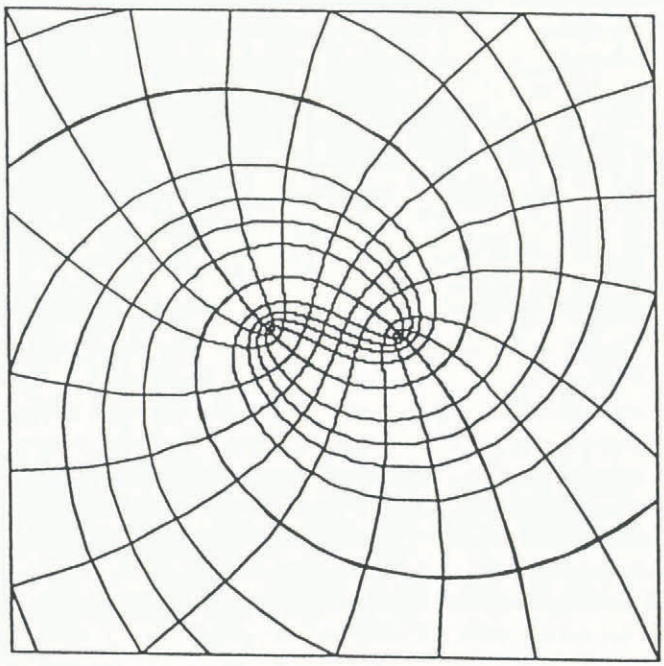

Fig. 3. When it is perturbed, the structurally unstable isotropic point of Figure 1b, with its pattern of principal strain-rate trajectories, splits into two, as illustrated here for $c' = 1$. Both points have the lemon pattern.

https://doi.org/10.3189/S0022143000015677 Published online by Cambridge University Press

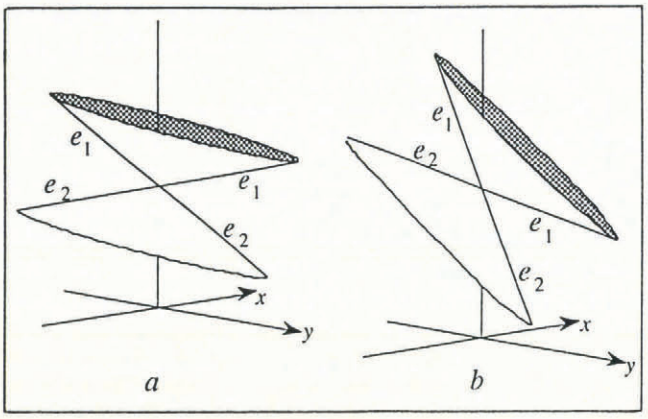

Fig. 4. The magnitudes of the principal strain rates e_1 and e_2 in the immediate neighbourhood of an isotropic point are represented as a function of position by the heights of these conical surfaces above the horizontal x,y plane. In (a) the contours of constant magnitude will be ellipses, while in (b) they will be hyperbolas.

An additional attribute of any isotropic point, independent of its singularity index, is its *contour property*. If the magnitudes of the principal strain rates at any point are denoted by e_1, e_2 $(e_1 \geq e_2)$, the contours of constant e_1 in the immediate neighbourhood of an isotropic point are either a set of ellipses or a set of hyperbolas. The same applies to the contours of constant e_2. Thus a given isotropic point can be classified as elliptic or hyperbolic. This comes about because the surfaces whose heights above the horizontal x, y plane are e_1 and e_2 are the two sheets of a cone. According to the orientation and angle of the cone, horizontal cross-sections are either ellipses (Fig. 4a) or hyperbolas (Fig. 4b).

Let us now examine the two isotropic points of Figure 3 from this point of view. It was shown in Nye (1991) that the distribution of the strain-rate tensor **e** has the local form

$$\mathbf{e} = \begin{pmatrix} K+\varepsilon_1+b(3x^2+y^2)+cxy & \varepsilon_2-\frac{1}{2}c(x^2-y^2)+2bxy \\ \varepsilon_2-\frac{1}{2}c(x^2-y^2)+2bxy & K-\varepsilon_1+b(x^2+3y^2)-cxy \end{pmatrix}. \quad (1)$$

Here, K is the unperturbed isotropic strain rate at the origin, ε_1 is a small constant specifying the perturbation, b and c are constants that define the unperturbed distribution and $\varepsilon_2 = -(c/2b)\varepsilon_1$. This is the most general possible local expansion of **e** about the origin up to quadratic terms. The x, y axes have been chosen so that the two isotropic points, after perturbation, lie on the x-axis at $x = \pm(-\varepsilon_1/b)^{\frac{1}{2}} = \pm\varepsilon$, say, the sign of ε_1 being chosen to make ε real. Now, in the tensor (1), subtract the isotropic strain rate K, divide through by ε_1 and scale the axes isotropically by putting

$$x = \varepsilon X, \qquad y = \varepsilon Y, \quad (2)$$

noting that none of these operations affects the form of the contour pattern. The result is the strain-rate tensor

$$\begin{pmatrix} 1-3X^2-Y^2-2c'XY & -c'(1-X^2+Y^2)-2XY \\ -c'(1-X^2+Y^2)-2XY & -1-X^2-3Y^2+2c'XY \end{pmatrix} \quad (3)$$

where $c' = c/2b$. In this form the isotropic points appear at $X = \pm 1$, $Y = 0$, and the only adjustable parameter is c'. $c' = 0$ corresponds to the unperturbed pattern of Figure 1a, that is, no spiral character.

It is now straightforward to plot the contour pattern by using the standard equations

$$e_1 = \tfrac{1}{2}(e_{11}+e_{22}) + \left(\tfrac{1}{4}(e_{11}-e_{22})^2 + e_{12}^2\right)^{\frac{1}{2}}$$

$$e_2 = \tfrac{1}{2}(e_{11}+e_{22}) - \left(\tfrac{1}{4}(e_{11}-e_{22})^2 + e_{12}^2\right)^{\frac{1}{2}}$$

where e_{11}, e_{22} and e_{12} are the elements of (3). Substitution of the values of e_{11}, e_{22} and e_{12} shows that the contour patterns for e_1 and e_2 are both symmetric about the X and Y axes. One can show analytically (Nye, 1991) that for $c' < (3)^{\frac{1}{2}}$ the contours near each isotropic point are hyperbolas, while for $c' > (3)^{\frac{1}{2}}$ they are ellipses. In nature, one would normally expect the former case because presumably c' would be small. For no perturbation, the circular symmetry ensures that the contours are concentric circles about the origin.

Figure 5a–d shows how the transition from circles to hyperbolas or ellipses comes about, for several values of c'. Because of the scaling, and its dependence on ε_1, the two isotropic points are always at the same point $X = \pm 1$, $Y = 0$. Therefore, the unperturbed pattern, namely circles, is to be seen at a large distance. For $c' = 0$, the contours of both e_1 and e_2 resemble ellipses at low resolution (Fig. 5a), but on magnification the region around (1,0) is seen to be hyperbolic, as expected (Fig. 5b). The contour through (1,0) for both e_1 and e_2 has a corner. For $c' = 1.7$, just less than the critical value $(3)^{\frac{1}{2}}$, the two arms of the corner have nearly closed up (Fig. 5c) and the contours are about to become locally parabolic. When they are exactly parabolic (not shown), the two isotropic points are joined by a single straight contour of e_2. For $c' = 3$ (Fig. 5d), the contours around (1,0) have become closed, in fact ellipses, as predicted, both for e_1 and e_2.

All this is made more intelligible by seeing the variation of e_1 and e_2 along the x-axis. Figure 6a shows the unperturbed strain rates for three values of c'. For each c', the curves for e_1 and e_2 are $y = 0$ sections through two paraboloids of revolution, which touch at $x = 0$, $y = 0$. The quadratic, rather than conical, contact between the two surfaces representing e_1 and e_2 is a further indication that this isotropic point is degenerate. Figure 6b is the corresponding section after perturbation. We are seeing the $y = 0$ section through two surfaces $e_1(x, y)$ and $e_2(x, y)$ which make conical point contact at the two isotropic points. The shading indicates the interior of each cone. The curves are parabolas, but now each curve represents e_1 for one part of its length and e_2 for the other part. It is clear that for $c' = 0$ horizontal sections will be hyperbolas, while for $c' = 3$ they will be ellipses. For the transition value $c' = (3)^{\frac{1}{2}}$ one of the parabolas is a horizontal straight line.

https://doi.org/10.3189/S0022143000015677 Published online by Cambridge University Press

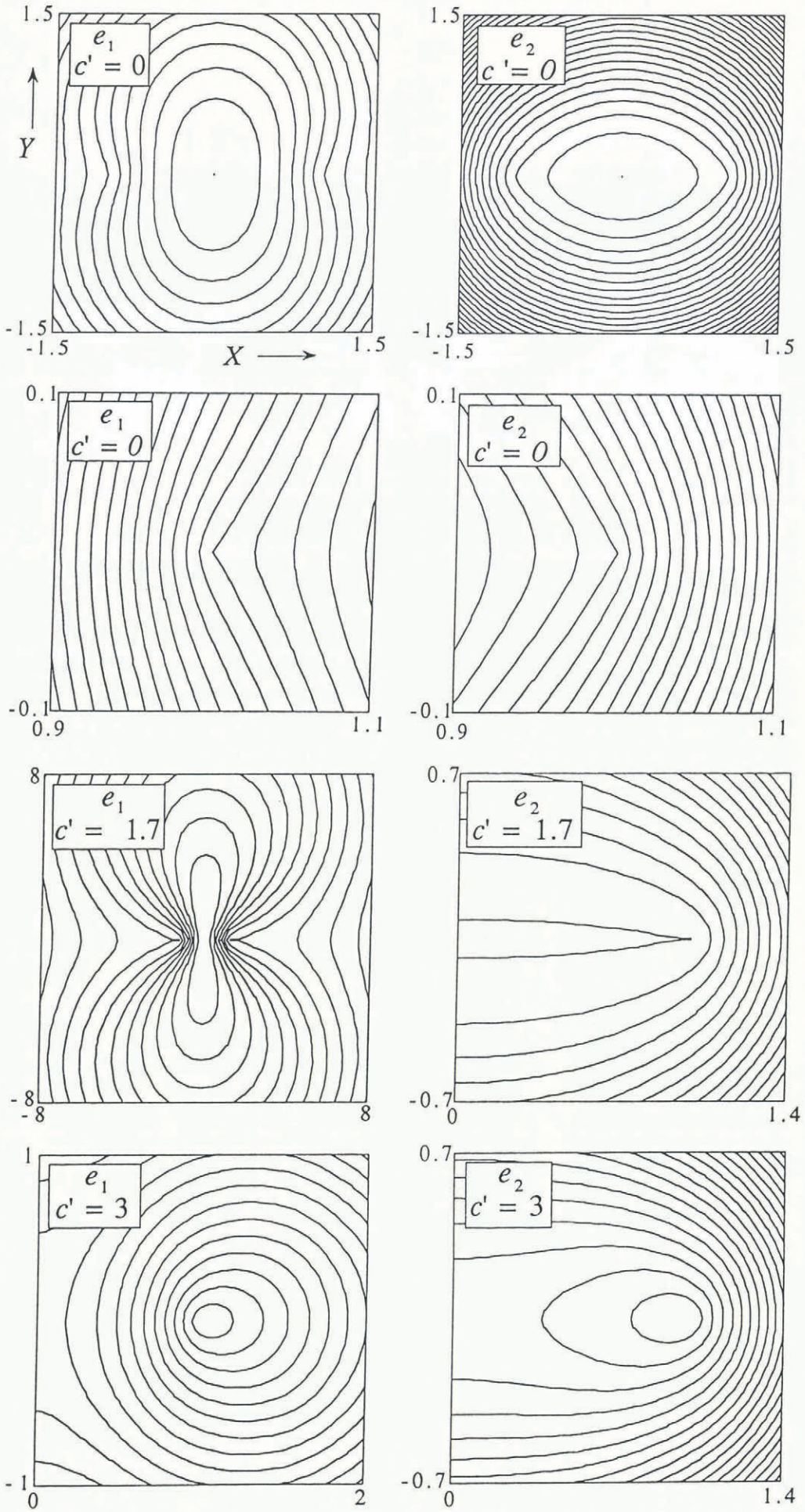

Fig. 5 a–d. Contour maps of the magnitudes of principal strain rates e_1 and e_2 for $c' = 0$, 1.7 and 3. Note the different scales of the diagrams.

https://doi.org/10.3189/S0022143000015677 Published online by Cambridge University Press

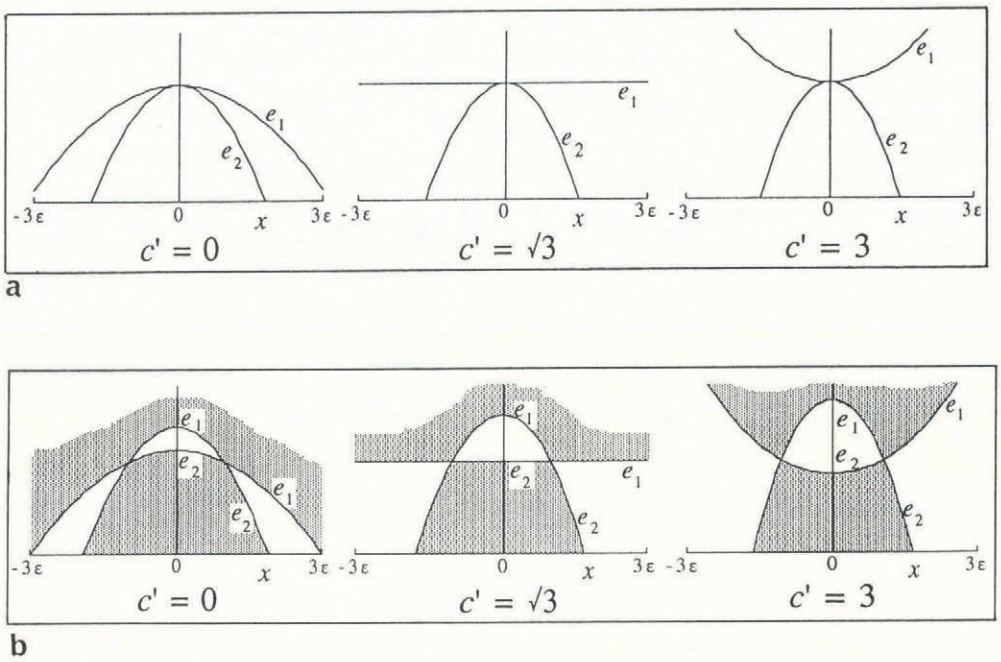

Fig. 6. Principal strain rates e_1 and e_2 plotted against x for y = 0. (a) Unperturbed, (b) perturbed. b has been chosen negative.

3. DISCUSSION

I remarked at the beginning that the generality of the results derived by topological methods is both a strength and a weakness. It would not be correct to say that the results are entirely non-quantitative — after all, the critical value $c' = (3)^{\frac{1}{2}}$ is certainly a quantitative result; but it is true that reasoning of this kind does not, of itself, provide estimates of distances or velocities or strain rates. Only models of the conventional kind can do this satisfactorily. For example, although topological reasoning predicts that the principal strain-rate trajectories around an isotropic point will invariably (this is its strength) have one of the three patterns of Figure 2, it does not say how large this local region will be. In practice, the answer to that question must depend on the amount of smoothing that has been applied, that is, it depends on the map scale used. With an appropriate map scale, the size of the "local" region around the isotropic point will usually be determined by the distance either to its nearest neighbour or to the boundary.

In the example of the splitting of a degenerate isotropic point there is an additional question that we have already alluded to: whether, for any particular ice-sheet summit, the two isotropic points indicated by first-order perturbation theory actually exist, or whether they have separated so far that they have already undergone further interactions. Once again, the scale of the map used must be an important factor, because the smaller the scale of the map the simpler the pattern of isotropic points will be, and the more likely we are to see the elementary pair.

REFERENCES

Berry, M. V. and J. H. Hannay. 1977. Umbilic points on Gaussian random surfaces. *J. Phys. A*, **10**(11), 1809–1821.

Nye, J. F. 1983. Monstars on glaciers. *J. Glaciol.*, **29**(101), 70–77.

Nye, J. F. 1990. Interpreting the field evidence of past ice sheets: structural stability and genericity. *Ann. Glaciol.*, **14**, 208–210.

Nye, J. F. 1991. The topology of ice-sheet centres. *J. Glaciol.*, **37**(126), 220–227.

The accuracy of references in the text and in this list is the responsibility of the author, to whom queries should be addressed.

MS received 1 July 1991 and in revised form 11 December 1991